



*J. Serb. Chem. Soc.* 75 (2) 271–282 (2010)  
JSCS–3959

## Preparation and characterization of a new carbonaceous material for electrochemical systems

ZI JI LIN<sup>1,2</sup>, XUE BU HU<sup>1,2</sup>, YONG JIAN HUAI<sup>1,2</sup> and ZHENG HUA DENG<sup>1,2\*</sup>

<sup>1</sup>Chengdu Institute of Organic Chemistry, Chinese Academy of Sciences, Chengdu, Sichuan 610041, and Graduate School of Chinese Academy of Sciences, Beijing, 100039 and <sup>2</sup>Zhongke Laifang Power Science & Technology Co., Ltd., Chengdu, Sichuan 610041, P.R. China

(Received 19 February, revised 4 June 2009)

**Abstract:** A new carbonaceous material was successfully prepared by the pyrolysis of scrap tire rubber at 600 °C under a nitrogen atmosphere. The physical characteristics of the prepared carbonaceous material were studied by scanning electron microscopy (SEM), X-ray powder diffraction (XRD) and X-ray photoelectron spectroscopy (XPS). It was proved that the carbonaceous material had a disordered structure and spherical morphology with an average particle size about 100 nm. The prepared carbonaceous material was also used as electrodes in electrochemical systems to examine its electrochemical performances. It was demonstrated that it delivered a lithium insertion capacity of 658 mA h g<sup>-1</sup> during the first cycle with a coulombic efficiency of 68 %. Cyclic voltammograms test results showed that a redox reaction occurred during the cycles. The chemical diffusion coefficient based on the impedance diagram was about 10<sup>-10</sup> cm<sup>2</sup> s<sup>-1</sup>. The pyrolytic carbonaceous material derived from scrap tire rubber is therefore considered to be a potential anode material in lithium secondary batteries or capacitors. Furthermore, it is advantageous for environmental protection.

**Keywords:** pyrolytic carbon; scrap tire rubber; carbonaceous materials; electrochemical performance; coulombic efficiency; chemical diffusion coefficient.

### INTRODUCTION

The lithium-ion battery has developed rapidly in the past decades due to its advantages of high electromotive force and high energy density. In today's commercial lithium-ion batteries, carbonaceous materials are widely used as the anodes. As compared with lithium metal, carbonaceous anodes reduce the formation of lithium dendrites on the surface of the anodes during the cycling process, which effectively enhances the safety and prolongs the cycle of lithium-ion batteries. In general, carbonaceous materials are classified into two groups: highly

\* Corresponding author. E-mail: zhdeng@cioc.ac.cn  
doi: 10.2298/JSC10020271L

graphitized carbons and slightly graphitized carbons of disordered structures. Graphitic carbons are the dominant anode material in today's lithium-ion technology because of their good characteristics of a relatively flat potential and stable structure upon cycling. However, the formation of graphitic carbons usually requires high reaction temperatures and their reversible capacities which, normally below  $372 \text{ mA h g}^{-1}$ , are limited compared with lithium metal.

Low-crystalline carbons, also named disordered carbons, have received considerable interest because of their appealing features, such as higher specific capacities of lithium insertion; good cycling performances; structural characteristics controllable by changing the organic precursors, heat-treatment temperature and soaking time.<sup>1,2</sup> Disordered carbons synthesized by the pyrolysis of organic precursors can accommodate much larger amounts of lithium than graphitic carbons, because disordered carbons contain predominantly planar hexagonal networks but lack extended graphitic crystallite ordering. Moreover, the short-sized graphite layers in disordered carbons are relatively facile for the insertion of lithium ions compared with graphitic carbons.<sup>3</sup>

Scrap tires are usually considered as waste materials. Owing to their flexible nature and resistance to degradation, under-grounding tires would occupy large volumes of land and tires tend to cause destabilization of compacted landfill sites. Scrap tires would also lead to significant fire hazards and generate high levels of pollution to the air, soil and waters. In fact, scrap tires may represent a source of many valuable products. According to recent management strategies that focus on valuable resources recycling and environmental protection, pyrolysis is regarded as one of the most promising techniques in terms of the recovery of valuable products from scrap tire rubber.<sup>4</sup>

Disordered carbons prepared by the pyrolysis of condensed aromatics<sup>5,6</sup> and a multitude of natural precursors<sup>7-11</sup> have been reported. These disordered carbons showed high initial insertion specific capacities and good electrochemical performance but low initial coulombic efficiencies. In this paper, the results of the structural characteristics and electrochemical performance of carbonaceous material pyrolyzed from scrap tire rubber are reported. The as-prepared carbonaceous material in the present study was designated as TRC. To evaluate the electrochemical properties of TRC, the widely used commercial powdered graphite carbons (abbreviated as CGP and F-0), activated carbon (abbreviated as AC) were used for comparative purposes.

## EXPERIMENTAL

### *Preparation of the carbonaceous material*

The scrap tire rubber employed in this work was in powdered form of particle size about 0.3 mm. A tube furnace was used to produce the carbonaceous material. Before pyrolysis, the rubber powder was washed with anhydrous ethanol. Subsequently, the above rubber precursor was heated at  $600 \text{ }^\circ\text{C}$  for 2 h in flowing nitrogen at a heating rate of  $2 \text{ }^\circ\text{C min}^{-1}$ . After natural

cooling to room temperature, the residual solid sample was mixed with a 1.0 M acetic acid solution in a 250 mL screw cap glass bottle to leach the inorganic elements to a minimum. The mixture was milled by magnetic force for 24 h and then end-over-end shaken for 6 h at room temperature. Afterwards, the mixture was filtered through a low-ash filter paper and then washed with distilled water until the pH value of the filtrate was neutral.

#### *Analytical and testing instruments*

SEM Images were obtained with a Hitachi X-650B microscope. The XRD data was collected between the scattering angles ( $2\theta$ ) 0 and 90° using a Rigaku D/Max 2550 powder diffractometer equipped with Cu-K $\alpha$  radiation source ( $\lambda = 0.15418$  nm). The XPS was collected on a VG Escalab MK II instrument.

#### *Assembly of cells and performance evaluation*

The electrochemical properties of various carbonaceous materials were evaluated with a lithium metal foil as the counter electrode. The working electrode was prepared by mixing TRC (or CGP, F-0 and AC), acetylene black and an aqueous binder LA132 (from Indigo, China) at a weight ratio of 87:5:8, in an appropriate amount of distilled water to make slurry. After mixing well, the slurry was pasted onto a 12  $\mu$ m copper foil and dried at 120 °C to give the electrodes. All electrodes were cut into disks with a diameter of 14.5 mm (thus the area of 1.65 cm<sup>2</sup>), pressed, dried at 90 °C under vacuum for 4 h, and weighed to determine the active mass of carbon.

All the operations on the cells assembly were realized in an argon-filled dry glove box. The electrolyte was 1.0 M LiPF<sub>6</sub> dissolved in a mixture of ethylene carbonate (EC), dimethyl carbonate (DMC) and ethylene methyl carbonate (EMC) with a volume ratio of 1:1:1. A porous Celgard 2400 polypropylene membrane was used as the separator. The constant current charge–discharge and room temperature cycling performance of the cells were tested on a Neware battery tester (China) and cyclic voltammograms (CVs) were measured using an Arbin Instrument (USA). Electrochemical impedance spectra (EIS) were investigated by a Solartron 1260/1287 (UK) impedance analyzer in the frequency range of 10<sup>-1</sup>–10<sup>6</sup> Hz.

## RESULTS AND DISCUSSION

### *SEM Characterization of the carbonaceous materials*

The SEM microphotographs of CGP, F-0, AC and TRC are shown in Fig. 1. The carbonaceous materials showed different morphologies. The SEM image of TRC revealed a spherical morphology and the TRC spheres were comparatively smooth with an average particle size of *ca.* 100 nm. According to Aurbach,<sup>12</sup> carbonaceous materials with a smoother surface give a better lithium-ion insertion/desertion performance. This is because a smooth surface is advantageous for the formation of an effective passivation layer. In addition, carbon spheres are thought to be beneficial for obtaining an improved performance because of their high pack density, low surface-to-volume ratio, good structural stability, *etc.*<sup>13</sup> Therefore, this morphological feature of the TRC material derived from the pyrolysis of scrap tire rubber is expected to be favorable for good cycling stability.

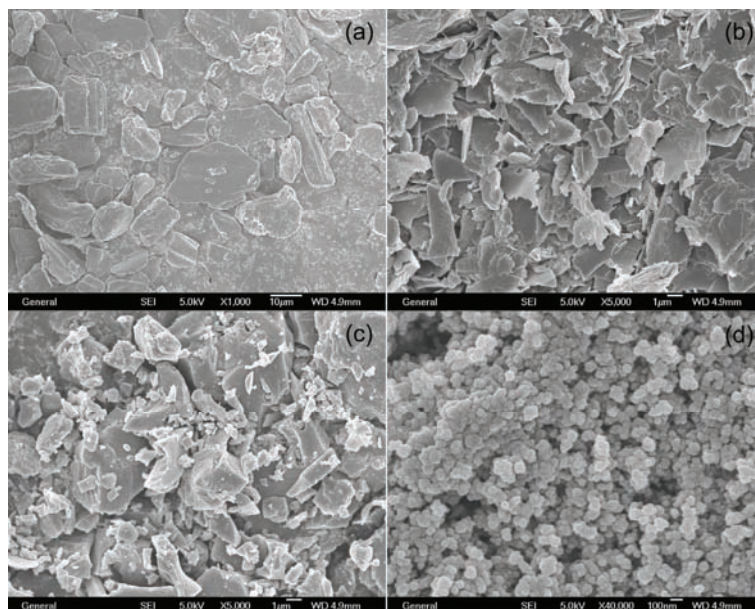


Fig. 1. SEM Images of a) CGP, b) F-0, c) AC and d) TRC.

### XRD Characterization

The XRD patterns of CGP, F-0, AC and TRC are presented in Fig. 2. As Sandí *et al.*<sup>14</sup> indicated, CGP and F-0 show a highly graphitized carbon structure, while AC and TRC display disordered carbon systems. The diffraction peak of (100) at around  $43^\circ$  indicates the presence of planar hexagonal cluster structures, while the broad reflection of (002) at around  $24^\circ$  indicates stacking of the graphite sheets in TRC, as shown in Fig. 2d. The  $d_{002}$  of TRC is about  $3.65 \text{ \AA}$ , which is a little larger than that of pure graphite carbon, as revealed in Figs. 2a and 2b. The larger interlayer distance of TRC is facile for the insertion and desorption of lithium ions and the retention the structural stability of TRC during cycles.

As indicated by Liu *et al.*,<sup>15</sup> the empirical parameter  $R$  can be used to estimate the concentration of nonparallel single layers of carbon in carbonaceous materials pyrolyzed at low temperatures. In the present study, the  $R$  value of TRC was found to be about 3.10. As shown in Figs. 2c and 2d, the  $R$  value of AC was higher than that of TRC, indicating more graphitized carbon single layers in TRC. The amount of the precursor loaded for pyrolysis is considered to be a condition for a large value of  $R$ . The reason is that large sample (more than 10 g precursor) when heat-treated can generate a higher partial vapor pressure of volatile organic products which may be able to redeposit in a process similar to the chemical vapor deposition (CVD) action. The capacity of a sample is correlated with

the value of  $R$  that lies on the fraction of the single layers. Samples with lower  $R$  values have more single layers and generally give a larger reversible specific capacity. For all single layers  $R = 1$ ,<sup>15</sup> as shown in Figs. 2a and 2b. Therefore, the single-layer fraction in TRC is small, which is one of the possible reasons that TRC has a relatively lower reversible specific capacity.

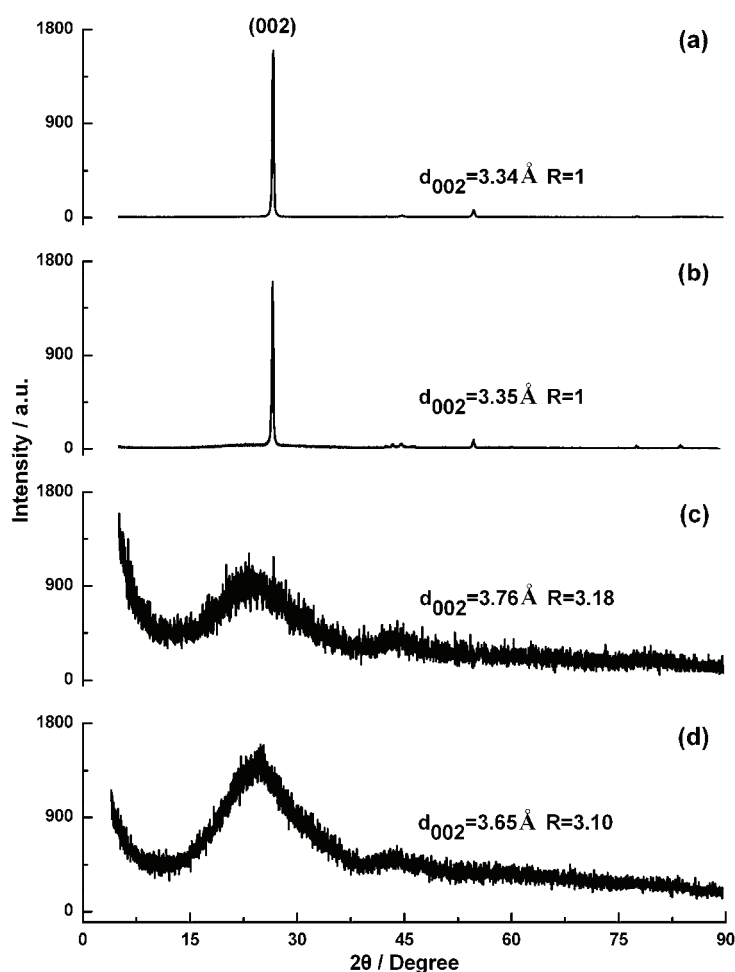


Fig. 2. XRD Patterns of a) CGP, b) F-0, c) AC and d) TRC.

#### XPS Measurements

The X-ray photoelectron binding energy spectrum of  $C_{1s}$  in TRC is given in Fig. 3. The spectrum shows that the TRC mainly consists of four kinds of carbon, including elemental carbon (C–C), phenol or ether (C–O), carbonyl (C=O) and carboxyl (COOH), which correspond to binding energies at 284.8, 286.2, 287.9

and 289.6 eV, respectively. Surface functional groups such as C–O, C=O and COOH were mainly formed during the pyrolysis process. As Ogihara *et al.* discussed,<sup>3</sup> these surface functional groups would cause a loss of reversible capacity because of their potential reactions with lithium.

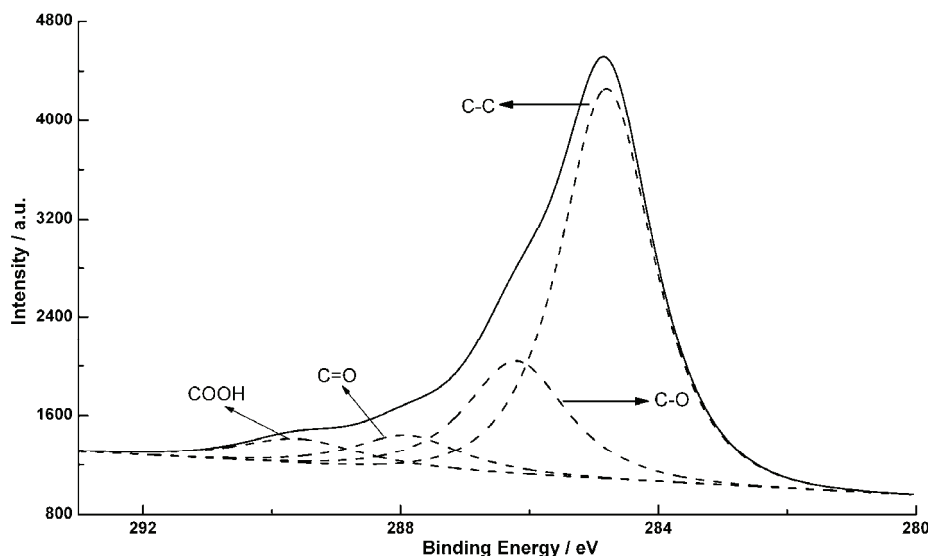


Fig. 3. X-Ray photoelectron binding energy spectrum of C1s in TRC.

#### Cyclic voltammetry

The CVs of CGP, F-0, AC and TRC are shown in Fig. 4 (1). The scan rate for all the electrodes was  $0.2 \text{ mV s}^{-1}$ . As can be seen from Fig. 4 (1), the four carbonaceous materials showed different electrochemical behaviors. The charge–discharge curves of CGP, F-0, AC and TRC, as shown in Fig. 4 (2), also display their different electrochemical properties. The CGP and F-0 electrodes exhibited the same oxidation–reduction behavior, *i.e.*, Li-ion insertion–extraction, in the electrodes. The AC electrode exhibited no redox peaks, which is due to the process of electrostatic adsorbing–desorbing of  $\text{PF}_6^-$  in AC. The TRC electrode exhibited two reduction peaks in the potential regions of 1.4–0.4 V and 0.4–0 V. The currents ( $i$ ) at 1.4–0.4 V varied almost linearly with the scan rate ( $v$ ), especially at the potentials of 0.6 and 0.4 V, as shown in Fig. 5. This result demonstrates a surface reaction behavior,<sup>16</sup> which is consistent with those of Ogihara.<sup>3</sup> In the potential region 1.4–0.4 V, a solid-electrolyte interface (SEI) film formed. The SEI films were mainly produced by the electrochemical reduction of solvent species at 1.2 V, the emphraxis of EC-solvated lithium on the carbonyl edges ( $\text{C}_{\text{edge}}=\text{O}$ ), and the reaction of lithium ions with  $\text{C}_{\text{edge}}=\text{O}$  to give the reversible redox reaction  $\text{C}_{\text{edge}}=\text{O}/\text{C}_{\text{edge}}\text{-OLi}$ .<sup>17</sup> Consequently, the high capacity in the po-



tential region of 1.4–0.4 V is the result of the electrochemically reversible redox of  $C_{\text{edge}}=O/C_{\text{edge}}\text{-OLi}$ , which is cyclable and occurs only on the electrode surface. In the potential region of 0.4–0 V, as suggested by other authors,<sup>18–20</sup> this is regarded as lithium ion insertion into the graphite layers ( $C_6\text{Li}$ ) and/or electrochemical deposition of metallic lithium clusters ( $\text{Li}^0$ ). Simultaneously, a LiF resistive film is formed irreversibly at around 0.2 V.<sup>17</sup>

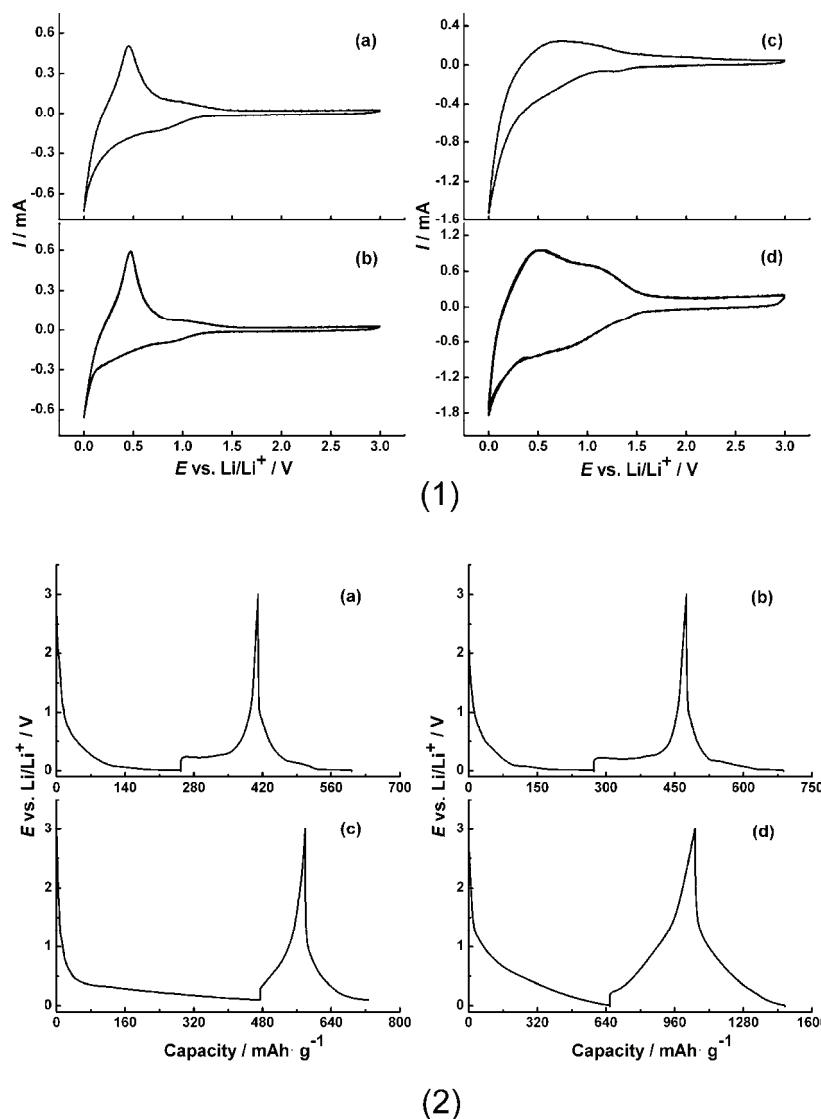


Fig. 4. 1) Cyclic voltammograms and 2) charge–discharge curves of a) CGP, b) F-0, c) AC and d) TRC.

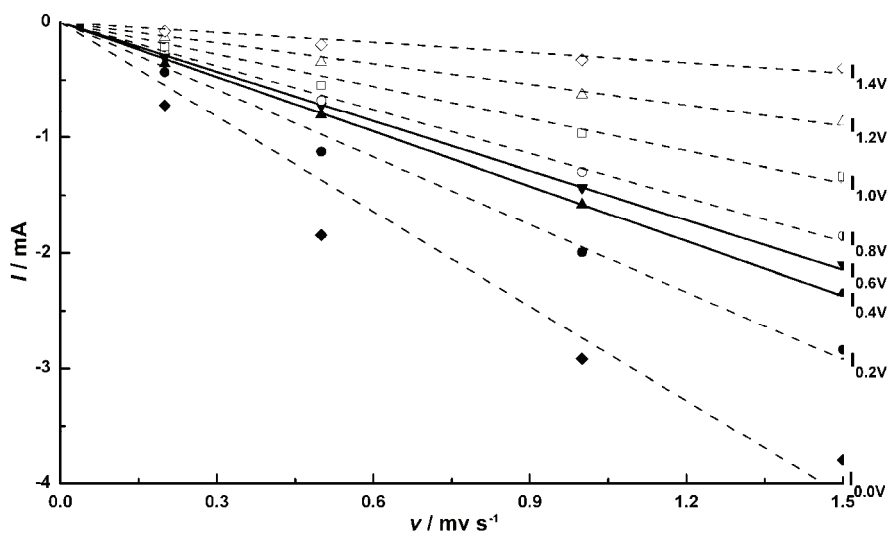


Fig. 5. Scan rate ( $v$ ) dependence of the current ( $i$ ) for TRC at potentials of 1.4, 1.2, 1.0, 0.8, 0.6, 0.4, 0.2 and 0.0 V.

### Cycling properties

The variations of the charge and discharge capacities with cycle number, together with the coulombic efficiency, for TRC are shown in Fig. 6. The cells were cycled between 0 and 3 V vs. Li/Li<sup>+</sup> at a current density of 0.45 mA cm<sup>-2</sup>. A

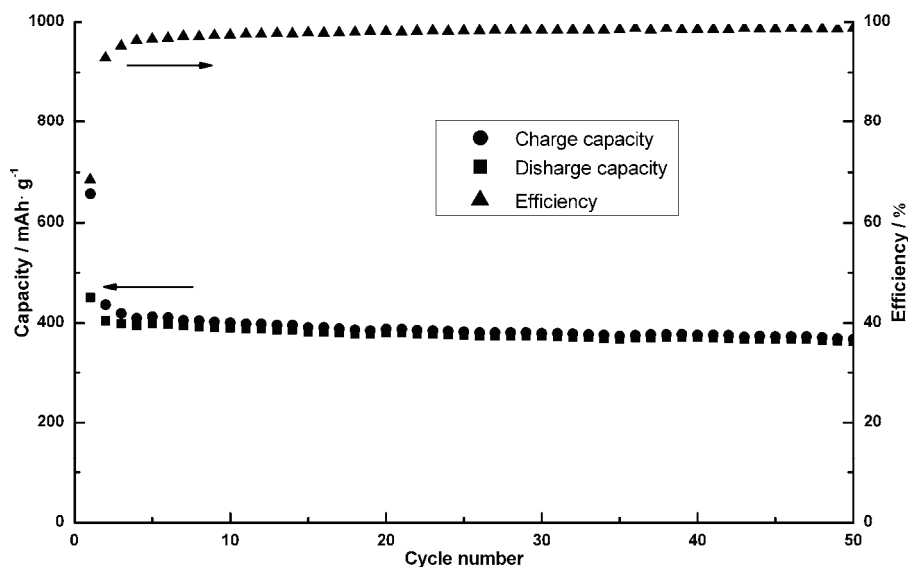


Fig. 6. Variation of the charge and discharge capacities with cycle numbers, together with the coulombic efficiency for TRC.



capacity of  $658 \text{ mA h g}^{-1}$  was obtained during the initial discharge with a coulombic efficiency of 68 %. The initial coulombic efficiency was much higher than that of many other carbonaceous materials obtained by pyrolysis.<sup>7,10,11,21,22</sup> The TRC electrode exhibited a rapid capacity fading in the first two cycles, although the irreversible capacities gradually decreased in the subsequent cycles. A sufficient passivation layer was not formed because of the structural characteristics of TRC and electrochemical parameters, such as large surface area, abundant functional groups, and/or large current density are thought to be the reasons. The low coulombic efficiencies of the first two cycles are considered to be caused by the fact that the applied current was consumed not only when lithium ions were inserted into the TRC during the discharge process, but also by other side reactions, such as solvent decomposition. After the 2<sup>nd</sup> cycle, the fading of both the charge and discharge capacities become slow and the coulombic efficiency reaches up to 95 %, which were because highly passivated surface films formed, the effect of side reactions abated and the structure of TRC became much more stable with cycling.

#### Impedance measurements

The impedance diagrams obtained for cells with a TRC electrode before cycling and after four cycles are shown in Fig. 7. The semicircles in the medium frequency region correspond to the process of insertion of lithium ions. The semicircle in the high frequency region for the cell after four cycles is considered to correspond to the formation of an SEI film on the electrode surface. The diagram

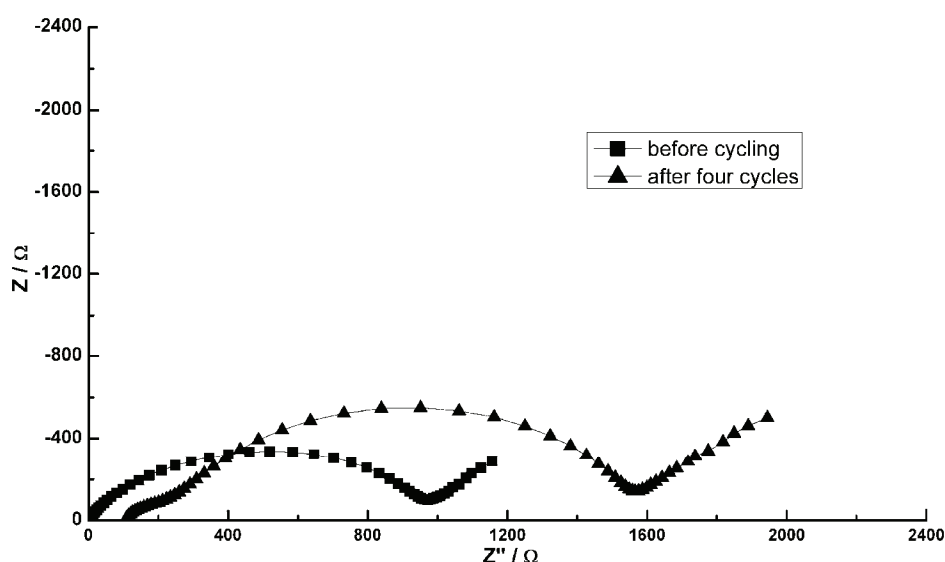


Fig. 7. Impedance diagram of the TRC electrode system before cycling and after four cycles.

also demonstrates that the impedance of the cell greatly increased upon cycling. This would be caused by the micro-exfoliation of the carbon particles during the repeated insertion-desertion process. As indicated by Levi *et al.*,<sup>23</sup> the micro-exfoliation would result in an increase of the surface area electrode and lead to a continuous reduction of the solvent species. As a result, the electrode becomes more covered by solution-reduced products and exfoliated carbon; hence the impedance of the cell increases. The chemical diffusion coefficient of lithium was calculated from the straight line of the impedance spectrum<sup>24</sup> shown in Fig. 7. This value corresponds to  $2.0 \times 10^{-10} \text{ cm}^2 \text{ s}^{-1}$ , which is larger than the value obtained by Sandí *et al.*<sup>14</sup>

### CONCLUSIONS

Scrap tire rubber was proved to be a suitable precursor for the production of carbonaceous electroactive materials for lithium-ion batteries. The prepared sample showed a disordered structure and spherical morphology with a relatively smooth surface and comparatively uniform particle size distribution. The higher chemical diffusion coefficient of lithium indicated the rapid transfer of lithium ions during cycling. As suggested by Aurbach *et al.*,<sup>25</sup> the structural characteristics of carbonaceous materials have an important influence on the voltage profile, reversibility and the final stoichiometry of the lithium-inserted carbon. The electrochemical performances of TRC were largely determined by its surface morphology and structural characteristics. A structure with a certain degree of crystallization and a certain number of pores is necessary for TRC to give a high capacity because the cavities in the TRC may be favorable for a greater accommodation of lithium ions. The disordered pyrolytic carbon TRC derived from scrap tire rubber showed a first-cycle coulombic efficiency of more than 65 %, which is much higher than other carbonaceous materials of the same family obtained from other precursors, although it exhibited a relatively low reversible capacity.

More importantly, not only the electrode materials could be obtained from scrap tire rubber by pyrolysis, but also the serious “black pollution” by scrap tires would be effectively solved by this method, which is thus advantageous for environmental protection.

### ИЗВОД

#### СИНТЕЗА И КАРАКТЕРИЗАЦИЈА НОВОГ УГЉЕНИЧНОГ МАТЕРИЈАЛА ЗА УПОТРЕБУ У ЕЛЕКТРОХЕМИЈСКИМ СИСТЕМИМА

ZI JI LIN<sup>1,2</sup>, XUE BU HU<sup>1,2</sup>, YONG JIAN HUAI<sup>1,2</sup> и ZHENG HUA DENG<sup>1,2</sup>

<sup>1</sup>Chengdu Institute of Organic Chemistry, Chinese Academy of Sciences, Chengdu, Sichuan 610041, and Graduate School of Chinese Academy of Sciences, Beijing, 100039 и <sup>2</sup>Zhongke Laifang Power Science & Technology Co., Ltd, Chengdu, Sichuan 610041, P.R. China

Синтетисан је нови угљенични материјал пиролизом отпадака аутомобилских гума на 600 °C у атмосфери азота. Физичке карактеристике угљеничног материјала су испитиване

скенирајућом електронском микроскопијом (SEM), дифракцијом X-зрака (XRD) и фотоелектронском спектроскопијом X-зрака (XPS). Показано је да материјал има неуређену структуру и сферну морфологију са просечном величином честица од око 100 nm. Синтетисани угљенични материјал је коришћен и као електрода у електрохемијским системима да би се испитале његове електрохемијске карактеристике. Резултати су показали да је капацитет интеркалације литијума 658 mAh/g током првог циклуса уз кулоновску ефикасност од 68 %. Цикличном волтаметријом је показано да се током циклуса одиграва редокс реакција. На основу импедансних мерења одређен је коефицијент дифузије литијума од око  $10^{-10}$  cm<sup>2</sup>/s. На основу ових резултата може се рећи да би се угљенични материјал добијен пиролизом отпадака аутомобилских гума могао користити као анодни материјал у литијумским батеријама, што би истовремено био и допринос очувању животне средине.

(Примљено 19. фебруара, ревидирано 4. јуна 2009)

#### REFERENCES

1. T. Zheng, Y. Liu, E. W. Fuller, S. Tseng, U. von Sacken, J. R. Dahn, *J. Electrochem. Soc.* **142** (1995) 2581
2. S. Yata, H. Kinoshita, M. Komori, N. Ando, T. Kashiwamura, T. Harada, K. Tanaka, T. Yamabe, *Synth. Met.* **62** (1994) 153
3. N. Ogihara, Y. Igarashi, A. Kamakura, K. Naoi, Y. Kusachi, K. Utsugi, *Electrochim. Acta* **52** (2006) 1713
4. F. Chen, J. Qian, *Waste Manage.* **23** (2003) 463
5. K. Sato, M. Noguchi, A. Demachi, N. Oki, M. Endo, *Science* **264** (1994) 556
6. A. Mabuchi, K. Tokumitsu, H. Fujimoto, T. Kasuh, *J. Electrochem. Soc.* **142** (1995) 1041
7. G. T. K. Fey, D. C. Lee, Y. Y. Lin, T. P. Kumar, *Synth. Met.* **139** (2003) 71
8. Y. Ohzawa, M. Mitani, J. Li, T. Nakajima, *Mater. Sci. Eng., B* **113** (2004) 91
9. G. T. K. Fey, Y. C. Kao, *Mater. Chem. Phys.* **73** (2002) 37
10. A. M. Stephan, T. P. Kumar, R. Ramesh, S. Thomas, S. K. Jeong, K. S. Nahm, *Mater. Sci. Eng. A* **430** (2006) 132
11. Y. J. Hwang, S. K. Jeong, J. S. Shin, K. S. Nahm, A. M. Stephan, *J. Alloys Comp.* **448** (2008) 141
12. D. Aurbach, H. Teller, E. Levi, *J. Electrochem. Soc.* **149** (2002) A1255
13. M. Yoshio, H. Wang, Y. Lee, K. Fukuda, *Electrochim. Acta* **48** (2003) 791
14. G. Sandí, R. E. Winans, K. A. Carrado, *J. Electrochem. Soc.* **143** (1996) L95
15. Y. Liu, J. S. Xue, T. Zheng, J. R. Dahn, *Carbon* **34** (1996) 193
16. L. M. Doubova, S. Daolio, A. D. Battisti, *J. Electroanal. Chem.* **532** (2002) 25
17. K. Naoi, N. Ogihara, Y. Igarashi, A. Kamakura, Y. Kusachi, K. Utsugi, *J. Electrochem. Soc.* **152** (2005) A1047
18. F. Chevallier, M. Letellier, M. Morcrette, J. M. Tarascon, E. Frackowiak, J. N. Rouzaud, F. Béguin, *Electrochem. Solid-State Lett.* **6** (2003) A225
19. K. Guérin, M. Ménétrier, A. Février-Bouvier, S. Flandrois, B. Simon, P. Biensan, *Solid State Ionics* **127** (2000) 187
20. I. Mochida, C. H. Ku, Y. Korai, *Carbon* **39** (2001) 399
21. Y. J. Hwang, S. K. Jeong, K. S. Nahm, J. S. Shin, A. M. Stephan, *J. Phys. Chem. Solids* **68** (2007) 182
22. I. Watanabe, T. Doi, J. Yamaki, Y. Y. Lin, G. T. K. Fey, *J. Power Sources* **176** (2008) 347
23. M. D. Levi, E. Levi, D. Aurbach, *J. Electroanal. Chem.* **421** (1997) 89

24. C. Ho, I. D. Raistrick, R. A. Huggins, *J. Electrochem. Soc.* **127** (1980) 343
25. D. A. Aurbach, Y. Ein-Elin, *J. Electrochem. Soc.* **142** (1995) 1746.